

The Role of Feature Enhanced Processing for Automatic Target Recognition using High Resolution Polarimetric SAR Data

Albertus van den Broek/ Philippe Steeghs/ Rob Dekker

TNO Physics and Electronics Laboratory

P.O. Box 96864

2509 JG The Hague

The Netherlands

vandenbroek/steeghs/r.j.dekker@fel.tno.nl

ABSTRACT

We have studied the effect of feature enhanced processing on the discrimination of targets in high-resolution polarimetric ISAR and SAR images. This is done by comparing feature-based classification results for original images and images which have been pre-processed to enhance target features. The data comprised four military targets: T72, ZSU23/4, T62, and BMP2. Images at a resolution of 10 cm have been extracted from the ISAR data for a complete aspect range of 360 degrees. The SAR images were taken from the MSTAR database with a resolution of 30 cm.

These images have been processed in order to enhance the geometrical delineation of the targets or to enhance point scattering. We have composed feature vectors out of individual features, which were extracted from the original and the enhanced images. The feature vectors are divided into three categories: radiometric, geometric and polarimetric. A maximum likelihood classifier was used to obtain discrimination results.

Knowledge about the aspect angle allows target discrimination per aspect angle interval, which will improve classification results. We have investigated the effect of feature enhanced processing on pose estimation. Pose estimation was obtained from the Radon transform of the original and enhanced imagery.

We found that the features extracted from enhanced images give slightly better results compared to features extracted from the original images. For the high-resolution enhanced ISAR data reasonable discrimination (about 80%) was obtained compared to the enhanced MSTAR data (about 60%), when radiometric and geometric features are used. Using the polarimetric features the discrimination results could be improved to 85%.

For aspect angle determination using the Radon transformation and for target discrimination per aspect angle interval no significant improvement was obtained using feature enhanced processing. The aspect angle could be determined up to an accuracy of 10-15 degrees, depending on the target. Discrimination per aspect interval using radiometric and geometric features shows results of 90% for the ISAR and 75% for the MSTAR images. Polarimetric information improves the results up to 97% for the ISAR images.

Paper presented at the RTO SET Symposium on "Target Identification and Recognition Using RF Systems", held in Oslo, Norway, 11-13 October 2004, and published in RTO-MP-SET-080.

1. INTRODUCTION

With the increasing use of UAVs for RSTA purposes also the interest in SAR imaging systems is growing, because of their unparalleled all-time and all-weather capability. In this context a study for the Dutch MOD was defined in which the role of SAR for ground surveillance is investigated. This study is carried out within the framework of the NATO/SET/TG14 research group, which focuses on robust acquisition of relocatable targets with advanced millimetre wave techniques. By participating in the group we have access to a database with high resolution SAR and ISAR data for various targets and scenes. This database was created and is maintained by the group to study automatic target recognition techniques in the millimetre wave domain. The US Army Research Laboratory (ARL) has contributed to the database with high-resolution (10cm) polarimetric ISAR data of four military targets at 35 Ghz. These data comprised two main battle tanks (T72, T62) an air defence unit (ZSU-23-4) and an infantry-fighting vehicle (BMP2). In a previous paper Van den Broek et al. [1] have studied the robustness of features against aspect variability for the purpose of target discrimination. They have shown that individual features show a strong variability as a function of aspect angle and cannot be used to discriminate between the targets irrespectively of the aspect angle. The use of feature vectors, which combine radiometric, geometric and if available polarimetric information, gives reasonable results. They also showed that the aspect angle could be determined sufficiently accurate using the Radon transformation, so that target discrimination per aspect interval is possible. Discrimination results per aspect interval are significantly higher up to 20% compared to results irrespectively of the aspect angle. We study here the influence of feature enhanced processing using the same data set and method as in Van den Broek et al. [1] by comparing the results from the original images and from the feature-enhanced images. The paper is organised as follows. In section 2 we describe the data. In section 3 we discuss feature enhanced processing. In section 4 we describe the features and the classification method followed by results. In section 5 we focus on pose estimation and in section 6 we give a summary.

2. DESCRIPTION OF THE DATA

2.1 High resolution polarimetric ISAR data

The ARL-ISAR measurements were performed with a fully polarimetric stepped frequency radar. The measured data are in the frequency domain and the spatial domain image is obtained through a 2-D inverse FFT [4]. Hamming weighting was applied to reduce the sidelobes of the impulse response. The following table summarizes the main properties of the data and images.

Table 1. ARL-ISAR data parameters

Band	Ka	Angle sampling interval	0.015°
Centre frequency	34.25 GHz	Nr. of samples (azimuth)	160
Bandwidth	1511.64 MHz	Resolution (azimuth)	10 cm
Frequency step	5.928 MHz	Polarisations	HH, HV, VH, VV
Nr. of samples (range)	256	Depression angle	10° (BMP2, T72, T62) and 12° (ZSU23-4)
Resolution (range)	10 cm	Incidence angle	80° (BMP2, T72, T62) and 78° (ZSU23-4)
Coherence interval	2.4°	Number of looks	Single Look

In this way a set of 397 fully polarimetric 10 cm resolution images was created covering the complete range of 360 degrees of aspect. This implies one image for every 0.9 degree of aspect. In figure 1 we show 10 cm ARL-ISAR images for the T62, T72, BMP and ZSU targets for one aspect angle.

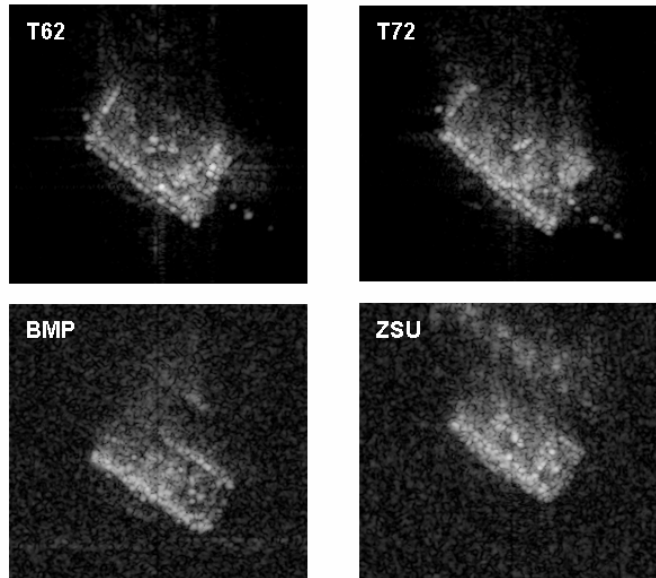


Figure 1. ARL-ISAR 10 cm resolution images for the T62, T72, BMP and ZSU targets.

2.2 MSTAR data

MSTAR data from the public database were used for comparison. These data were taken from data collection 1 (September 1995) and data collection 2 (November 1996). Data were collected at X-band, HH polarisation with about 30 by 30 cm resolution for various aspect angles covering the complete circle of 360 degrees. The depression angle of the selected data was 15 degrees. The MSTAR data comprised 275, 195, 196 and 276 aspect angles for the T62, T72, BMP and ZSU targets respectively. See Table 2 for further details.

Table 2. MSTAR data

Target	MSTAR data collection	Type
T62	data collection #2, scene 1	T62
T72	data collection #1	T72 variant SN 812
BMP	data collection #1	BMP-2 variant SN 9563
ZSU	data collection #2, scene 1	ZSU 23/4

We use the results from the MSTAR data for comparison with the results from the ARL-ISAR data. The comparison is not straightforward since there are differences in elevation angle (15 degrees versus 12/10 degrees) and the frequency band (Ka band versus X-band) used. In Figure 2 we show MSTAR data for the T62, T72, BMP and ZSU targets for one aspect angle.

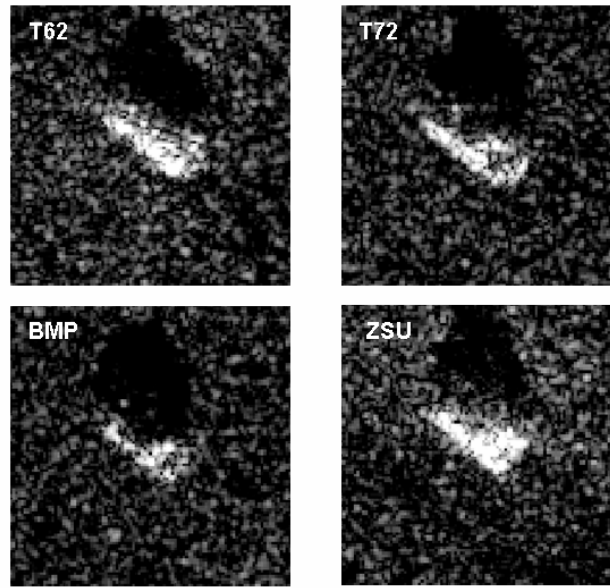


Figure 2. MSTAR 30 cm resolution images for the T62, T72, BMP and ZSU targets.

3. FEATURE ENHANCED PROCESSING

Following Çetin et al. [3] feature-enhanced image formation is achieved through an optimization process. The objective of this optimization is to find an estimate of the SAR reflectivity field \mathbf{f} from the measurement \mathbf{g} by minimizing the objective function:

$$J(\mathbf{f}) = \|\mathbf{g} - \mathbf{T}\mathbf{f}\|_2^2 + \lambda_1 \|\mathbf{f}\|_k^k + \lambda_2 \|\mathbf{D}|\mathbf{f}|\|_k^k. \quad (1)$$

Here $\|\cdot\|_k^k$, denotes the l_k norm, \mathbf{T} is a complex-valued SAR observation operator, \mathbf{D} is a 2-D derivative operator, $|\mathbf{f}|$ denotes the vector of magnitudes, and λ_1, λ_2 are scalar parameters. The first term in the objective function is a data fidelity term. The second and third term introduce prior information regarding the field \mathbf{f} into the optimization problem. Each of these terms aims at enhancing a particular feature. The second term can be interpreted as an energy type constraint on the solution. This term enhances dominant point-like features and suppresses artifacts. The derivative term results in a variability constraint on the solution and as a result leads to reduction of the variability in more or less homogeneous regions of the field. The parameters λ_1 and λ_2 can be chosen such that their relative magnitude emphasizes a particular feature. In this case we straightforwardly have chosen $\lambda_1=1, \lambda_2=0$ for *point enhancement* and $\lambda_1=0, \lambda_2=1$ for *region enhancement*. The choice k determines the properties of the prior function (the l_k -norm). For the first case $k=1$ and for the second case $k=1.5$ is chosen. The point enhanced processing obviously aims at enhancing the point features in the images and can be used to get a better separation of point scattering versus background scattering and if a finer grid is used to enhance the resolution (superresolution). The region enhanced processing aims at enhancing homogeneous regions in the image

and can be used to better extract the target outline, and to obtain homogenous backscatter within the target box. It also suppresses the background backscatter so that a complete separation of target and backscatter pixels is possible. Figure 3 shows an example of the result before and after feature enhanced processing of the T72 target in the MSTAR database.

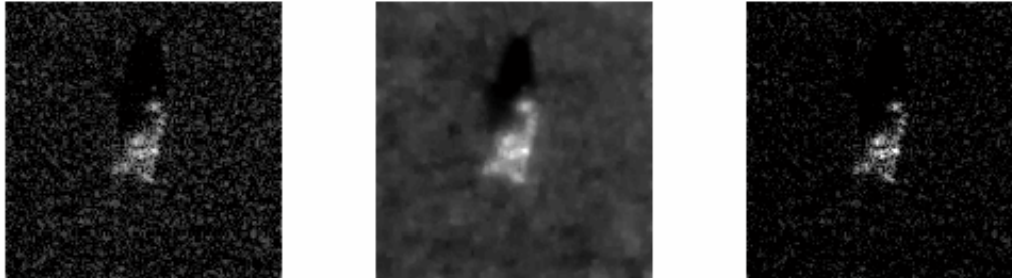


Figure 3. MSTAR data of T72 before (left) and after feature enhanced processing (centre: region enhanced, right: point enhanced).

4.0 TARGET DISCRIMINATION METHOD

4.1 Feature extraction

We selected three classes of features: radiometric, geometric and polarimetric. For each class three features were identified, which are expected to give independent information and are characteristic for the class they belong. Table 3 summarises the features used.

Table 3. Categories of features used

Radiometric		Geometric		Polarimetric	
<i>MEAN</i>	mean intensity	<i>AREA</i>	area of target	<i>HHHV</i>	polarimetric (HH/HV) power ratio
<i>CVAR</i>	coefficient of variation	<i>NN</i>	neighbour number	<i>EVEN</i>	percent odd
<i>WFR</i>	Weighted rank fill ratio	<i>LAC</i> or <i>FF</i>	lacunarity index or fill factor	<i>ODD</i>	percent even

As a basis to calculate the feature values we first used a CFAR detector [7] to detect target pixels. To obtain so-called CFAR masks we used dB scaled imagery and the CFAR constant was chosen halfway the maximum and the average background of the dB scaled images. Separate results for the CFAR were obtained for the original and feature enhanced processed images. Figure 4 shows examples of the CFAR masks and the corresponding images. For the original imagery obviously only one kind of CFAR mask is available while for the feature enhanced imagery two additional masks are available. In the latter case the

CFAR mask from region enhanced imagery is used, except for the feature *NN*, where the CFAR mask for the original imagery is used and for the feature *WFR*, where the CFAR from the point enhanced imagery is used. In case of enhanced imagery the *LAC* feature is replaced by the *FF* feature (see below).

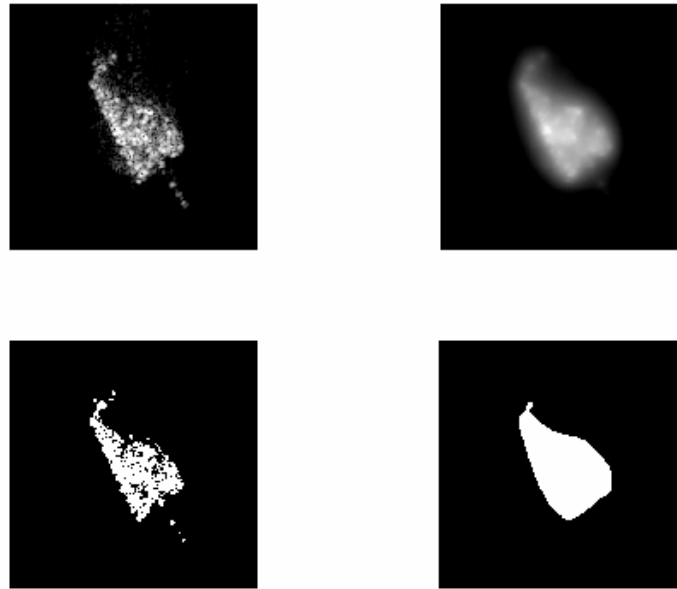


Figure 4. Top: ARL-ISAR T72 image (original: left and region enhanced: right). Bottom: corresponding detected CFAR masks.

Below we give a short description of the features.

MEAN: The mean (μ) of the power of the detected target pixels, which indicates how bright the target appears in the image.

CVAR: The normalized variance of the power of the detected target pixels indicates how smooth or not the scattering is distributed over the target and is defined by

$$cv = \frac{\sigma^2}{\mu^2}. \quad (2)$$

WFR: This measure is defined as the ratio of the sum of the power of the N brightest pixels, and the sum of power of all detected pixels [6]. For the 10 cm resolution images we took $N=75$ and for the 30 resolution images we took $N=10$. This feature measures the relative amount of scattering due to 'hot spots'.

AREA: The number of detected target pixels. This feature clearly indicates the geometric extent of the target.

NN: The neighbour number is a measure for the spatial distribution of the CFAR detected target pixels [2].

The number is defined by total number of neighbour pixels of all detected pixels normalized by the total number of detected pixels. This feature is a kind of texture measure indicating how well detected pixels are lumped together.

LAC: The lacunarity index is a textural feature that can discriminate between differently appearing surfaces with the same fractal dimension [8]. It is calculated by counting the number of detected pixels within an $n \times n$ moving window (we use here $n=3$). For the resulting moving-window filtered image the coefficient of variation is calculated following Equation 2, only for non-zero values of the detected pixels. This figure gives the lacunarity index and is a measure of the variation in lumpiness of the detected pixels. In other words the feature measures whether the detected pixels form a regular pattern (low value) or an irregular pattern (high value). Obviously, this feature only gives significant information when enough pixels are detected and the resolution is high enough.

FF: The fill factor indicates the fraction of pixels within the CFAR mask from the region enhanced imagery that belong to the CFAR mask of the original images. This feature is used in stead of the lacunarity index in case of feature enhanced imagery.

HHHV: This polarimetric measure is defined as the ratio of total power from the detected pixels in the HV image and the HH image. Note that the pixels are detected on using the HH image. A similar quantity using the HH and VV image is less useful since the HH and VV power are usually strongly correlated.

ODD and EVEN: These polarimetric measures refer to odd and even bounce scattering and are defined by

$$Odd = \frac{\sigma_{hh} + \sigma_{vv} + 2 \operatorname{Re}(\rho)}{2}, \quad (3)$$

$$Even = \frac{\sigma_{hh} + \sigma_{vv} - 2 \operatorname{Re}(\rho)}{2} + 2\sigma_{hv}, \quad (4)$$

where σ is the backscattering coefficient for the various polarisations and ρ is the correlation coefficient of the HH and VV polarisation. The feature percent odd is defined as the percentage of detected pixels for which odd bounce scattering dominates. A pixel is said to be dominated by odd bounce scattering when the odd bounce scattering is at least twice as large as the even bounce scattering. The feature percent even is similar, but now with the even bounce scattering dominating.

Using the method described in the previous section we have produced a database of 9x397 features for the 4 targets in the ARL-ISAR data for both the images without and with feature enhanced processing. For the non-polarimetric MSTAR data only 6 features (radiometric and geometric) could be extracted for the original and the feature enhanced imagery. In Figure 5 we show as example the *AREA* feature as a function of aspect angle for ARL-ISAR images without (left) and with (right) region enhanced processing.

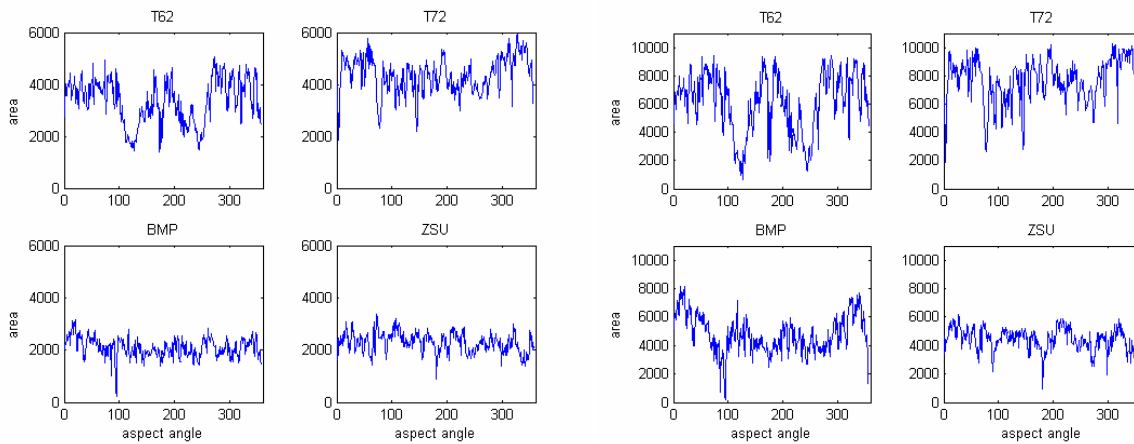


Figure 5. AREA feature as function of aspect angle for ARL-ISAR images (left) without and (right) with feature (region) enhanced processing.

4.2 Classification method

It is clear from figure 4 that the individual features can vary significantly especially near aspect angles of 0° , 90° , 180° , and 270° . These aspect angles coincide with observing the targets head-on, sideways or from behind. The capability to discriminate the targets irrespective of the aspect angle is generally low. Either there is large variation, or the more stable features are not very distinctive. This means that one individual feature is never capable of discriminating a target from the other targets irrespective of the aspect angle. In order to study how well we can discriminate the four targets from each other we compose feature vectors with the features extracted in the previous section as the constituting elements. The following 5 categories of feature vectors are used:

$$\begin{aligned}
 \text{radiometric:} &= [MEAN, CVAR, WFR]^T \\
 \text{geometric:} &= [AREA, NN, LAC]^T \\
 \text{polarimetric:} &= [HHHV, EVEN, ODD]^T \\
 \text{generic:} &= [MEAN, CVAR, WFR/FF, AREA, NN, LAC]^T \\
 \text{generic_pol:} &= [MEAN, CVAR, WFR/FF, AREA, NN, LAC, HHHV, EVEN, ODD]^T.
 \end{aligned}$$

The feature vector containing the geometric and radiometric features is called *generic* since it can always be extracted from SAR data, regardless whether the data are polarimetric or not. Of course these geometric and radiometric features only contain significant information when enough pixels can be found over the geometric extent of the target, implying that the resolution should be sufficiently high. The *generic_pol* feature vector obviously only applies to fully polarimetric data.

For the four targets we have constructed multi-variate target distributions where the elements of the distribution are the feature vectors at the various aspect angles. The number N corresponds to the number of aspect angles in the data-sets. The dimension of the multi-variate target distribution equals the number of elements in the feature vector used.

For each target distribution we calculated the mean feature vector and also the covariance matrix according to

$$\mu_j = \frac{1}{N} \sum_{i=1}^N \vec{x}_i, \tag{5}$$

$$\Sigma = \frac{1}{N} \sum_{i=1}^N (\vec{x}_i - \vec{\mu}_j)(\vec{x}_i - \vec{\mu}_j)^T, \tag{6}$$

where N is the number of aspects used and j indicates the T62, T72, BMP or ZSU target. Using these quantities we can now for each target and each aspect image calculate discriminant functions such as

$$d_j(\vec{x}_i) = (\vec{x}_i - \vec{\mu}_j)^T \Sigma_j^{-1} (\vec{x}_i - \vec{\mu}_j) + \log(|\Sigma_j|), \tag{7}$$

where i is the aspect angle index and j is the target index. The discriminant function is derived from the Bayes' decision rule, which also takes into account the a priori probability. Since this probability is the same for each target, the a priori probability has been omitted here. This is called maximum likelihood discrimination [5]. Note that the discriminant function is only working well under the assumption of normal distributions. Using a feature vector for the 4 targets, we assign the target for which the discriminant function is a minimum. This procedure is repeated for every aspect angle. Next, we compute confusion matrices indicating percentages of correctly and erroneously classifications. Using this method we have produced results for all 5 categories of features vectors.

In table 4 we show the confusion matrices for the *generic* feature vector for the ARL-ISAR and MSTAR data, both for the original and feature enhanced images. In table 5 we give the average percentages of correction classification (PCCs) for all feature vectors and the four cases (ARL-ISAR original, ARL-ISAR enhanced, MSTAR original, MSTAR enhanced). Since the MSTAR data are not polarimetric only three categories of feature vectors has been studied for these data.

Table 4. Confusion matrix for feature vector category *generic*

ARL-ISAR					MSTAR				
<i>Original image</i>					<i>Original image</i>				
	T62	T72	BMP	ZSU		T62	T72	BMP	ZSU
T62	80	18	1	1	T62	15	23	27	35
T72	34	66	0	0	T72	7	42	37	13
BMP	0	0	86	14	BMP	1	4	91	4
ZSU	0	0	20	80	ZSU	9	8	5	78
Average Pcc 78					Average Pcc 57				
<i>Feature enhanced</i>					<i>Feature enhanced</i>				
	T62	T72	BMP	ZSU		T62	T72	BMP	ZSU
T62	80	18	1	1	T62	25	34	4	36
T72	31	69	0	0	T72	8	66	18	9
BMP	0	0	93	7	BMP	1	12	85	3
ZSU	0	0	12	88	ZSU	14	15	1	70
Average Pcc 82					Average Pcc 61				

Table 5. Average PCCs

	ARL-ISAR		MSTAR	
	Original image	Feature enhanced	Original image	Feature enhanced
<i>Radiometric</i>	54	50	36	32
<i>Geometric</i>	63	69	48	51
<i>Polarimetric</i>	38	41	-	-
<i>Generic</i>	78	82	57	61
<i>Generic pol</i>	85	86	-	-

If we inspect the confusion matrices for the ARL-ISAR data we find that regardless of the feature enhanced processing most of the confusion is between the T72 and T62 targets, which is not surprising, since both are main battle tanks. For the MSTAR data most confusion is found between T62 and ZSU, and between T72 and BMP. Here, feature enhanced processing helps to reduce the confusion between T72 and BMP. The average PCCs in table 5 indicate that only the geometric feature vector gives a reasonable discrimination between the targets with an average PCC of 69% and 51% for the ARL-ISAR and MSTAR data, respectively. Feature enhanced processing helps to improve the results, especially for the ARL-ISAR data. The *generic* feature vector gives an average PCC of 82% and 61% for the ARL-ISAR and MSTAR data, respectively. Again, feature enhanced processing helps to improve the results, although this improvement is small. Best results (86%) are obtained when polarimetric information is included. In this case no significant improvement is found when feature enhanced processing is applied.

5.0 ASPECT ANGLE DETERMINATION

5.1 Radon transformation

For the goal of aspect determination we consider the Radon transformation of an image (the Radon transform). The Radon transformation of an image $f(x,y)$ is defined as

$$g(\rho, \theta) = \iint f(x, y) \delta(\rho - x \cos \theta - y \sin \theta) dx dy, \quad (8)$$

where δ denotes the Dirac delta function, θ is the rotation angle and ρ is the spatial axis parameter. Ideally a target in an image can be considered as a rectangular shape. The Radon transformation of an image containing such a shape will show a band, with peaks at the angle, for which the rectangle is seen along its long axis. Determination of the maximum in the Radon transformation image therefore gives the aspect angle. This method works well when the backscatter in the target box is homogeneous. However strong point scattering will also give strong peaks in the Radon transform and can hamper an accurate determination of the aspect angle. Also strong sidelobes due to strong scatterers will give erroneous values, typically 0 (180) or 90 (270) degrees. We use therefore images in log (dB) scaling, which suppress variation in backscattering. Figure 6 shows an example of a 10 cm ARL-ISAR image and its Radon transform. Using the method described here we determined the aspect angle for the four targets in original and feature enhanced imagery. For the latter case we used the region enhanced imagery. We also used the CFAR masks obtained from the original and region enhanced imagery to determine the aspect angle. Within the scope of method these masks have the advantage that they are homogeneous but on the other hand are lacking many other target characteristics (see figure 6).

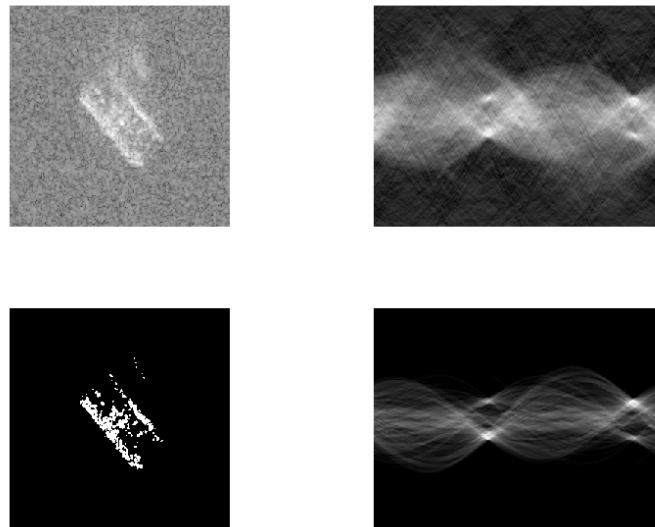


Figure 6. ARL-ISAR image (top left) and its Radon transform (top right), CFAR mask (bottom left) mask and its Radon transform (bottom right).

Note that with this method of aspect angle determination we cannot make distinction between head and rear of the targets. The values therefore are always between 0 and 180 degrees. In figure 7 we have plotted the values found against the actual values for the T72 target in the ARL-ISAR and MSTAR images. This is done for the four cases: original image dB scaled (image Radon), region enhanced image dB scaled (region enh. Radon), CFAR mask from original image (image CFAR Radon), and CFAR mask from region enhanced image (region enh. CFAR Radon). Comparison is done at about every 5 degrees in the complete 360 degrees of angle range.

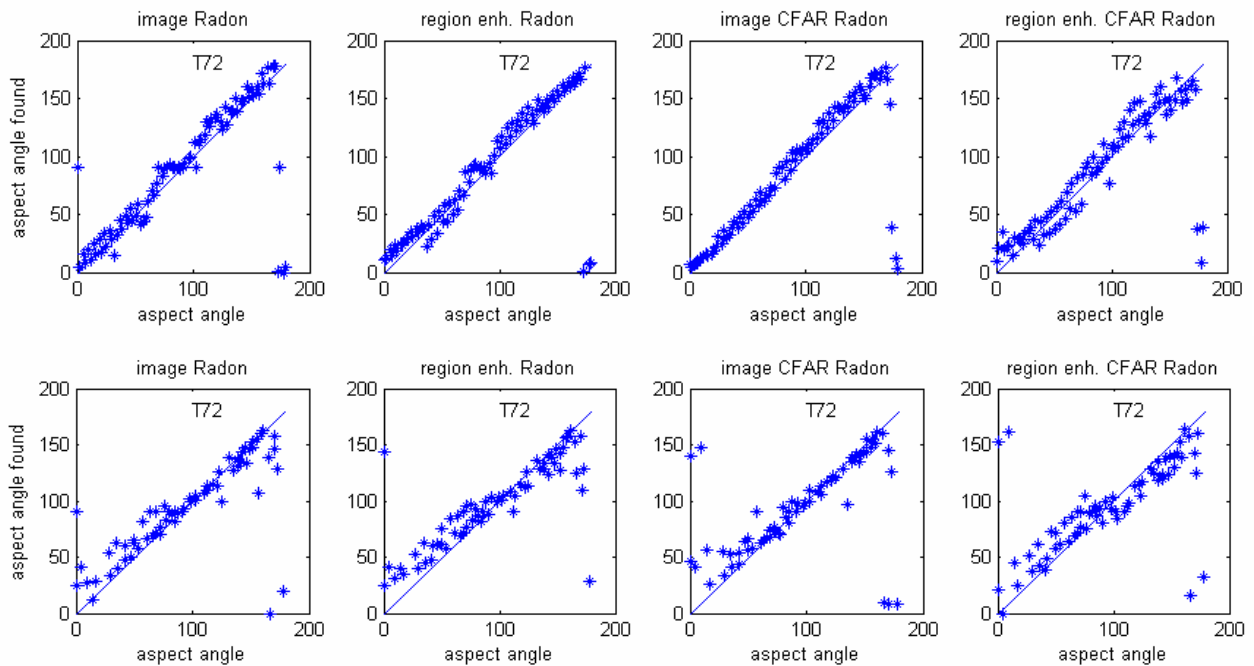


Figure 7. Aspect angles determined with Radon transforms versus the true aspect angle for the T72 target and the four cases. Top: ARL-ISAR and bottom: MSTAR.

To compare the results we calculated the root mean square (RMS) error between the values found and the actual values for the aspect angles. These are summarized in table 6 for the T62, T72, BMP and ZSU targets and the four cases considered.

Table 6. RMS errors in aspect angle determination using Radon transforms

	ARL-ISAR				MSTAR			
	image Radon	region enhanced Radon	image CFAR Radon	region enhanced CFAR Radon	image Radon	region enhanced Radon	image CFAR Radon	region enhanced CFAR Radon
T62	31	9	6	14	37	26	20	14
T72	16	9	10	13	19	19	17	17
BMP	15	9	11	9	24	16	8	12
ZSU	15	17	13	21	36	30	15	22
Average	19	11	10	14	29	23	15	16

Inspection of the average RMS values in table 6 shows that the MSTAR values are larger compared to those for the ARL-ISAR data. This is confirmed by figure 7 where more spread in the data is visible for the MSTAR case. The most accurate aspect angle determination is found when CFAR masks are used. Both CFAR masks based on original and region enhanced imagery are suitable for this purpose with slight better results for the original images. Using CFAR masks the aspect angle can be determined with an accuracy of somewhat larger than 10 degrees for the ARL-ISAR data and about 15 degrees for the MSTAR data. From table 6 it is clear that also target characteristics play a role. For example, aspect angle determination of the ZSU target is less accurate compared to the BMP target, probably due to strong specular reflections which have an effect on the location of the maximum in the Radon transform.

5.2 Target discrimination per aspect interval

In the previous section we have shown that aspect determination is possible with an accuracy of 10-15 degrees. This allows target discrimination per aspect interval, with dimensions in the order 30 degrees or more. In small aspect angle intervals feature values are more stable as a function of aspect angle, so that we overcome the variability of the features against aspect angle and can increase the percentage of correct classification. We divided the full aspect range of 360 degrees into 8 following aspect angle intervals (see figure 8):

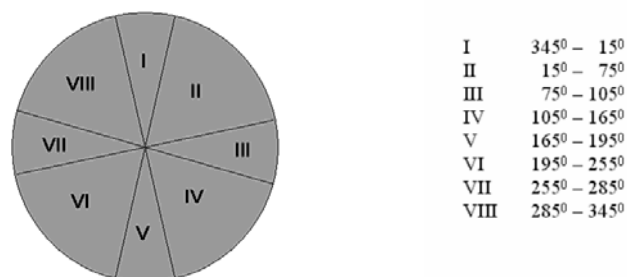


Figure 8. Overview of aspect angle intervals used.

These aspect intervals are chosen such that we can separate high backscatter (vehicle viewed head-on, sideways or from behind) and lower backscatter (vehicle viewed obliquely). Following section 4.2 we use feature vectors and covariance matrices and compute the discriminant functions following equation 7, but now per aspect interval. We obtain confusion matrices for the four targets per aspect interval and for the four cases considered in section 4.2 cases (ARL-ISAR original, ARL-ISAR enhanced, MSTAR original, MSTAR enhanced). Like in table 5 we give in table 6 the average percentages of correct classification averaged over the 8 intervals for the different feature vectors. Figure 9 shows the behavior of the feature vector *generic* as function of aspect interval.

Table 7. Average PCCs

	ARL-ISAR Original image	ARL-ISAR Feature enhanced	MSTAR Original image	MSTAR Feature enhanced
<i>Radiometric</i>	69	63	50	43
<i>Geometric</i>	79	68	61	61
<i>Polarimetric</i>	51	56	-	-
<i>Generic</i>	90	91	74	75
<i>Generic pol</i>	96	97	-	-

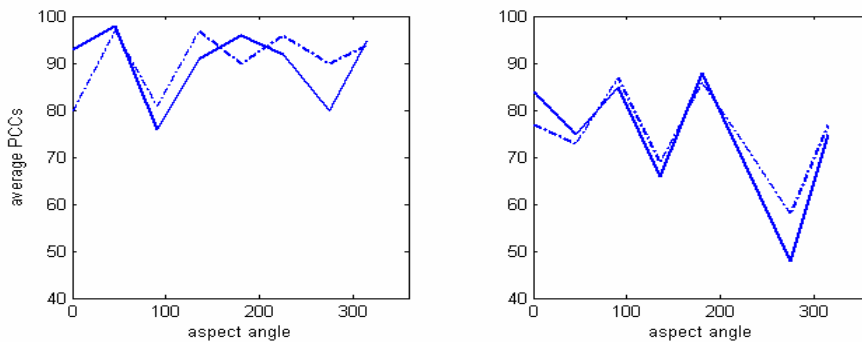


Figure 9. Average PCCs using the *generic* feature vector. To the left the results for the ARL-ISAR data and to right the results for MSTAR data are shown. The solid line is for the original images and the dotted for the feature enhanced images

The results in table 7 show that the average PCCs are significantly higher those in table5, both for the ARL_ISAR data as well as for the MSTAR data. The increase is typically 10%. There is no significant difference when feature enhanced processing is applied. The *generic* feature vector, which can be used for non-polarimetric data now gives a PCC of 90% for ARL-ISAR data and 75% for the MSTAR data. Especially when the resolution is high enough (10 cm ARL-ISAR data) and when also polarimetric information is used almost complete separation is obtained between the targets (97%). The results for the *generic* feature vector as a function of aspect angle in figure 9 show somewhat lower PCCs when the targets are viewed head-/tail-on or sideways. This is especially true at 270 degrees for the MSTAR data. This may be due to higher double bounce scatter between target and the ground, which is less discriminative. Again the difference between the results from original and feature enhanced imagery is small as a function of aspect angle interval.

6.0 SUMMARY

In this study we have evaluated the role of feature enhanced processing for the discrimination of targets in high-resolution SAR images. The feature enhanced processing aims at enhancing the point features in the images to get a better separation of point scattering versus background scattering (point enhancement), and at enhancing homogeneous regions in the image to better extract the target outline (region enhancement). We used four military targets: T62, T72, BMP and ZSU and images from 2 data-sets: ARL-ISAR (10 cm resolution) and MSTAR (30 cm resolution). We evaluated the discrimination of targets using feature vectors consisting of three categories: radiometric, geometric and polarimetric, extracted from two kinds of images: original and feature enhanced. To obtain results we used a maximum likelihood classifier.

As a first case we studied discrimination of targets irrespective of the aspect angle. Best results are obtained when all feature vector categories are combined, i.e. the radiometric and geometric category, and if available the polarimetric category and when feature enhanced processing is applied. In case of the combined radiometric and geometric feature vector, percentages of correct classification of about 80% could be obtained for the ARL-ISAR data and 60% for the MSTAR data. The use of feature enhancement helps to improve the percentages of correct classification by about 5%.

As a second case we have studied target discrimination per aspect angle interval. In practice this implies that the aspect angle has to be determined. We used the Radon transformation for this purpose. We found that the best way to do this is the use of target CFAR masks as input for the Radon transformation. We found typical accuracies of 10-15 degrees. In this case feature enhanced processing does not substantially improve the results. Discrimination results per aspect interval are significantly better compared to discrimination irrespective of aspect angle. We found percentages of correct classification up to 97% when radiometric, geometric and polarimetric features are used for ARL-ISAR data. When only radiometric and geometric features are used typical average percentages of correct classification of 90% for the ARL-ISAR data and 75% for the MSTAR data are found. Also, in this case feature enhanced processing did not have much effect on the results.

Concluding we can say that feature enhanced processing helps to improve discrimination results when no pose estimation is available. However, in this study feature enhanced processing does not help to obtain more accurate aspect angle information or to obtain better discrimination results per aspect interval. For this study we have chosen one particular way to extract and to process features. Feature enhanced processing opens more possibilities to handle features and this comparative study was not intended to optimize feature extraction and processing using feature enhanced imagery. Also, feature enhanced processing enables the enhancement of point scatterers, target extent, while reducing the background, which is clearly an advantage for visual inspection and interpretation.

7.0 REFERENCES

- [1] A.C. Broek, van den, R.J. Dekker, T.P.H. Steeghs, "Robustness of Features for Automatic Target Discrimination in High Resolution Polarimetric SAR Data", *Algorithms for Synthetic Aperture Radar Imagery X, Proc. of SPIE, Vol. 5095, 2003*, pp. 242-253.
- [2] A.C. van den Broek, R.J. Dekker, W.L. van Rossum, A.J.E. Smith, and L.J. Ewijk, "Feature extraction for automatic target recognition in high resolution and polarimetric SAR imagery", *TNO report, FEL-00-A2366, 2001*.
- [3] M. Çetin, W.C. Karl, and D.A. Castañon, "Analysis of the Impact of Feature-Enhanced SAR Image on ATR Performance", *Proc. of the SPIE Conference on Algorithms for SAR imagery, IX, vol.4742, Orlando, FL, April 2002*

- [4] C.C. Chen and H.C. Andrews, "Multifrequency Imaging of Radar Turntable Data", *IEEE Trans. on Aerosp. Electron. Syst.*, Vol. 16, No. 1, pp. 15-22, 1980.
- [5] R.O. Duda and P.E. Hart, *Pattern Classification and Scene Analysis*, John Wiley and Sons, New York, 1973.
- [6] D.E. Kreithen, S.D. Halversen, and G.J. Owirka, "Discriminating Targets from Clutter", *Lincoln Laboratory Journal*, Vol. 6, No. 1, pp. 25-52, 1993.
- [7] L.M. Novak and S.R. Hesse, "On the performance of order-statistics CFAR detectors", *IEEE Conference Record of the 25th Asilomar Conference on Signals, Systems and Computers*, Vol.2, pp. 835-840, 1991.
- [8] Plotnick, R.E., Gardner, R.H., and O'Neill, R.V., 1993, Lacunarity indices as measures of landscape texture, *Landscape Ecology*, Vol. 8, 201-211.

